Molecular Crystals and Liquid Crystals Science and Technology. Section A. Molecular Crystals and Liquid Crystals

Publication details, including instructions for authors and subscription information:
http://www.tandfonline.com/loi/gmcl19

Banana-Shaped or Rod-Like Mesogens? Molecular Structure, Crystal Structure and Mesophase Behaviour of 4,6-Dichloro-1,3-Phenylene Bis[4-(4-n-Subst.-Phenyliminomethyl) Benzoates]

W. Weissflog [a], Ch. Lischka [a], S. Diele [a], G. Pelzl [a], I. Wirth [a], S. Grande [b], H. Kresse [a], H. Schmalfuss [a], H. Hartung [a] & A. Stettler [a]

[a] Martin-Luther-Universität Halle-Wittenberg, Institut für Physikalische Chemie, Mühlpforte 1, D-06108, Halle

[b] Universität Leipzig, Fakultät für Physik und Geowissenschaften, Linnéstraβe 5, D-04103, Leipzig, Germany

Version of record first published: 24 Sep 2006

To cite this article: W. Weissflog, Ch. Lischka, S. Diele, G. Pelzl, I. Wirth, S. Grande, H. Kresse, H. Schmalfuss, H. Hartung & A. Stettler (1999): Banana-Shaped or Rod-Like Mesogens? Molecular Structure, Crystal Structure and Mesophase Behaviour of 4,6-Dichloro-1,3-Phenylene Bis[4-(4-n-Subst.-Phenyliminomethyl) Benzoates], Molecular Crystals and Liquid Crystals Science and Technology. Section A. Molecular Crystals and Liquid Crystals, 333:1, 203-235

To link to this article: http://dx.doi.org/10.1080/10587259908026006

Mol. Cryst. Liq. Cryst., Vol. 333, pp. 203-235
Reprints available directly from the publisher
Photocopying permitted by license only

Banana-Shaped or Rod-Like Mesogens? Molecular Structure, Crystal Structure and Mesophase Behaviour of 4,6-Dichloro-1,3-Phenylene Bis[4-(4-n-Subst.-Phenyliminomethyl) Benzoates]

W. WEISSFLOG[a*], CH. LISCHKA[a], S. DIELE[a], G. PELZL[a], I. WIRTH[a], S. GRANDE[b], H. KRESSE[a], H. SCHMALFUSS[a], H. HARTUNG[a] and A. STETTLER[a]

[a]Martin-Luther-Universität Halle-Wittenberg, Institut für Physikalische Chemie, Mühlpforte 1, D-06108 Halle and [b]Universität Leipzig, Fakultät für Physik und Geowissenschaften, Linnéstraße 5, D-04103 Leipzig, Germany

(Received August 27, 1998; In final form August 27, 1998)

Terminally alkyl- and alkyloxysubstituted 4,6-dichloro-1,3-phenylene bis[4-(phenyliminomethyl)benzoates] have been synthesized and studied by optical microscopy, differential scanning calorimetry, NMR spectroscopy, X-ray diffraction and dielectric measurements. Surprisingly, nematic and smectic phases are observed, although comparable bisesters of resorcinol and monochlororesorcinol exhibit B phases typical for banana-shaped mesogens. It could be proved by NMR investigations in the liquid crystallinen state that the molecules have a nearly rod-like shape. Dielectric measurements indicate a rotation around the molecular long axis as known from calamitic mesogens, which is clearly distinguished from the behaviour of bent molecules. Obviously, substitution of the central phenyl ring of the bent 1,3-phenylene bis[4-(4-n-alkyloxyphenyliminomethyl)benzoates] by two chlorine atoms causes a markedly change of the molecular shape resulting in nearly calamitic mesogens. These results are supported by single crystal structure studies, which allow the precise determination of the molecular structure and packing in the solid state.

Keywords: liquid crystals; banana-shaped mesogens; NMR; X-ray diffraction; dielectric measurements; molecular structure; crystal structure

* Author of correspondence.

1. INTRODUCTION

The ferro- (or antiferro-) electric switching of achiral compounds reported at first by Takazoe et al. [1] stimulated a lot of synthetic work and physical investigations to elucidate the relationships between the chemical constitution and the electrooptical properties. The molecules of those compounds exhibit a bent shape, also designated as banana-shaped in the recent literature. That shape is one important precondition for packing in layers with C_{2v} symmetry to obtain a polarization within the layers [2]. Together with a tilt of the bent molecules within the layers a breaking of the symmetry can result in a formation of chirality in the bulk phase [3]. Meanwhile we know that five or more different mesophases can be formed by bent mesogens, all characterized by a layer structure without in-plane order [4]. However, only two of them are electrooptically switchable [5]. Furthermore, all these mesophases formed by banana-shaped molecules are not miscible with mesophases known from calamitic mesogens. For this reason the field of bent-shaped mesogens should be discussed as a new liquid crystal subfield.

To study the relationships between the structure of bent mesogens, the existence of the novel B phases and their physical properties, especially the electrooptical properties, the chemical constitution of the molecules can be varied concerning the number and substitution of aromatic rings, the length and types of terminal groups, the type and direction of connecting groups, but also concerning the symmetry and flexibility of the whole molecules. An important aspect will be the question in which way the bend angle between the two half-parts of the molecule is influenced.

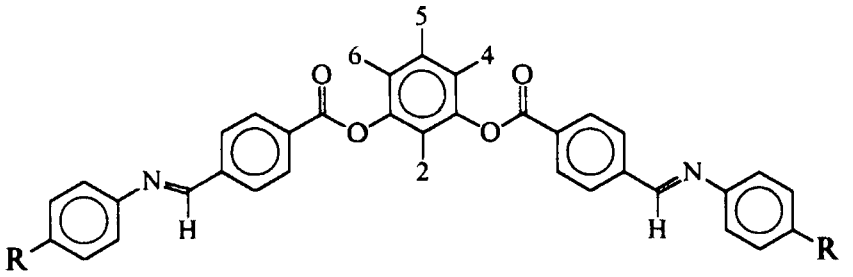

In the present paper it shall be shown, how a minor change of the chemical constitution leads to a dramatic alteration of the conformation of the molecules resulting in the loss of the new B phases. Starting from the "classical"

banana-shaped 1,3-phenylene bis[4-(4-n-alkyloxyphenyliminomethyl)benzoates], having H-atoms in the position 2,4,5,6 [1], the introduction of small substituents or groups into the central 1,3-phenylene ring can be of an important influence. Here, the influence of two chlorine atoms situated in the positions 4 and 6, will be investigated concerning the structure of mesophases as well as of the crystal structure, the conformation of the molecules and the dynamic behaviour in electric fields.

2. MATERIALS

Because of the azomethine groups in the molecules esterification of 4,6-dichlororesorcinol with 4-(4-n-subst.-phenyliminomethyl)benzoic acids **1a-g** was performed by means of dicyclohexylcarbodiimide in the presence of dimethylaminopyridin in dichloromethan according to Steglich et al. [6]. The substituted benzoic acids used as intermediates were prepared by condensation of the appropriate 4-n-alkyloxy- or 4-n-alkylanilines with 4-formylbenzoic acid under nitrogen in ethanol. These two-ring benzoic acids **1a-g** are liquid crystalline themselves as expected.

4-(4-Subst. -phenyliminomethyl)benzoic acids 1a-g

4-n-Alkoxyaniline (50 mmol) or 4-n-alkylaniline, resp., and 4-formylbenzoic acid (50 mmol) were dissolved in absolute ethanol (250 ml). The mixture was refluxed under nitrogen for 8 hours. After cooling the product precipitated was filtered off. The acid was recrystallized twice from ethanol, yields 65–80%. The phase transition behavior is summerized in Table I.

The analytical data are given for the 4-(4-n-decyloxyphenyliminomethyl)benzoic acid:

Elemental analysis:	$C_{24}H_{31}NO_3$; Mm 381.49
calculated:	C=75.56; H=8.19; N=3.67;
found	C=75.38; H=8.41; N=3.70

^{1}H-NMR: 200 MHz ($CDCl_3$) $\delta = 8.54$ (s, 1H, CH=N), 8.15 (d, 2H, Ar-H, J=8.4 Hz), 7.97 (d, 2H, Ar-H, J=8.4 Hz), 7.3 (d, 2H, Ar-H, J=8.8 Hz), 6.92 (d, 2H, Ar-H, J=8.9 Hz), 3.96 (t, 2H, OCH_2, J = 6.6 Hz), 1.63 (m, 2H, OCH_2CH_2), 1.25 (m, 14H, CH_2), 0.86 (m, 3H, CH_3).

TABLE I Phase transition temperatures (°C) and enthalpies [kJ/mol] of the 4-(4-subst.-phenyliminomethyl)benzoic acids **1a-g**

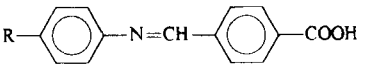

No.	*R*	*cr*		*smC*	*N*		*is*
1a	$C_6H_{13}O$	·	189	· 258	·	266	·
			[16.0]	[3.0]		[8.5]	
1b	$C_7H_{15}O$	·	190	· 255	·	261	·
			[14.5]	[-]		[16.3]	
1c	$C_8H_{17}O$	·	183	· 258	·	261	·
			[16.0]	[-]		[19.7]	
1d	$C_9H_{19}O$	·	180	· 260	-		·
			[16.2]	[19.6]			
1e	$C_{10}H_{21}O$	·	175	· 259	-		·
			[29.1]	[33.3]			
1f	$C_{12}H_{25}O$	·	155	· 255	-		·
			[30.8]	[35.8]			
1g	$C_{14}H_{29}$	·	132	· 232	·	242	·
			[10.8]	[0.97]		[13.8]	

4,6-Dichloro-1,3-phenylene bis[4-(4-subst. -phenyliminomethyl)benzoates] 2a-g

4-(4-Subst.-phenyliminomethyl)benzoic acid **1** (4mmol) and 4,6-dichlororesorcinol (2mmol) were dissolved in absolute dichloromethane (100 ml), dicyclohexylcarbodiimide (5mmol) and a small amount dimethylaminopyridine as catalyst were added. The mixture was stirred at room temperature for 48 hours. The solution was filtered off and the solvent evaporated. The products were recrystallized manyfold from ethanol/dimethylformamide and after that purified by flash chromatography on neutral aluminiumoxide with chloroform as eluent and, finally, recrystallized from toluene/heptan. Yields: 45–62 %. The phase transition temperatures are listed together with the transition enthalpies in Table II.

The analytical data are given for the octyloxy derivative **2c**:

Elemental analysis:	$C_{50}H_{54}Cl_2N_2O_6$, M=849.89;
calculated:	C=70.66; H-6.40; Cl=8.34; N=3.30;
found:	C=70.39; H=5.90; Cl=8.68; N=3.45

^{1}H-NMR: (200MHz; $CDCl_3$) δ = 8.56 (s, 2H, CH=N), 8.28 (d, 4H, Ar-H, J=8.5 Hz), 8.03 (d, 4H, Ar-H, J=8.3 Hz), 7.64 (s, 1H, Ar-H), 7.41 (s, 1H, Ar-H), 7.27 (d, 4H, Ar-H, J=8.8 Hz), 6.93 (d, 4H, Ar-H, J=8.9 Hz), 3.97 (t, 4H, OCH_2, J = 6.6 Hz), 1.78 (m, 4H, OCH_2CH_2), 1.28 (m, 20H, CH_2), 0.88 (m, 6H, CH_3).

TABLE II Phase transition temperatures (°C) and transition enthalpies [kJ/mol] of the 4,6-dichloro-1,3-phenylene bis[4-(4-n-alkyloxyphenyliminomethyl)benzoates] **2a-g**

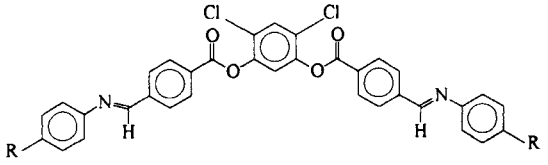

No.	*R*	*cr*		smC̃		*smC*		*N*		*is*
2a	$C_6H_{13}O$	·	127	-				·	165	·
			[46.2]						[1.8]	
2b	$C_7H_{15}O$	·	115	-				·	153	·
			[35.9]						[1.3]	
2c	$C_8H_{17}O$	·	126	-				·	148	·
			[45.7]						[0.9]	
2d	$C_9H_{19}O$	·	106	(·	88)			·	143	·
			[13.9]		[1.6]				[0.5]	
2e	$C_{10}H_{21}O$	·	111 1	(·	97)			·	140	·
			[43.8]		[-]				[1.5]	
2f	$C_{12}H_{25}O$	·	111	·	111–113 ·		121	·	137	·
			[47.2]		[-]		[0.9]		[1.9]	
2g	$C_{14}H_{29}$	·	94	·	98–100 ·		117	-		·
			[33.5]		[-]		[6.1]			

3. EXPERIMENTAL

The optical investigations were performed using a polarizing microscope (Leitz Orthoplan and Nikon) equipped with a Linkam hot stage (THM 600/S). The thermal behaviour was investigated with a Perkin-Elmer DSC 7 differential scanning calorimeter.

To carry out X-ray studies in the mesophases the orientation of the samples has been achieved either by applying a magnetic field where the samples were hold

in glass capillaries of 1 mm diameter or by annealing of a droplet on a glass surface.

The scattering of oriented samples were recorded by a 2D detector (HI Star, Siemens AG). Besides this the scattering of non-oriented samples has been measured with a Guinier equipment (System 400 HUBER Diffraktionstechnik GmbH).

The NMR measurements were performed using a Bruker MSL 500 spectrometer at a field of 11.7 T. The samples were put in a standard 5 mm tube. The proton decoupled ^{13}C spectra at 125 MHz are well resolved. The amplitude of the decoupling field in liquid crystalline phases was as low as possible (0.6–0.8 mT) to avoid a heating of the sample. Simple pulse excitations and cross-polarization experiments with HP- or WALTZ-decoupling are used. In the former case an offset of the proton frequency (0.5 – 3 kHz against methylene resonance) influences the efficiency of the decoupling and helps in the identification of the lines.

Dielectric investigations were carried out in a double plate capacitor ($A = 2\ cm^2$, $d = 0.02$ cm) using the HP 4192A and the Solartron Schlumberger SI 1260 impedance analyzers. For the compounds under investigation the appearence of a nematic phase did allow to orient the director by an external magnetic field of 0.6 T.

Single crystals of **2c** suitable for the crystal structure determination by X-ray investigations were obtained by recrystallization from methanol. The intensity data were measured on a Stoe STADI4 diffractometer equipped with an Oxford Cryostream low-temperature apparatus at 200 K using graphite-monochromated MoK_α radiation ($\lambda = 0.71073$ Å) in the ω/θ-scan mode. Lattice parameters were derived by a least-squares treatment of the setting angles for 70 reflections. Data correction was carried out applying Lorentz and polarization corrections but neglecting absorption effects. The structure was solved by direct methods and refined by full-matrix least squares on F^2 with anisotropic displacement parameters for non-hydrogen atoms. The hydrogen atoms were located based on geometric considerations and treated according to the riding model during refinement with isotropic displacement parameters.

All calculations were done by means of programs SHELXS-86 [7] and SHELXL-93 [8]. The figures of molecular structure and packing were plotted using the Siemens XP/PC program [9]. Further details of the crystal structure determination are available on request from the Fachinformationszentrum Karlsruhe, Gesellschaft für wissenschaftlich-technische Information mbH, D-76344 Eggenstein-Leopoldshafen, on quoting the depository number CSD-410105, the names of the authors and the journal citation.

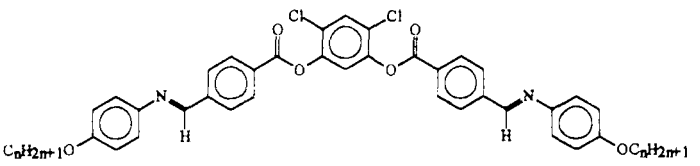

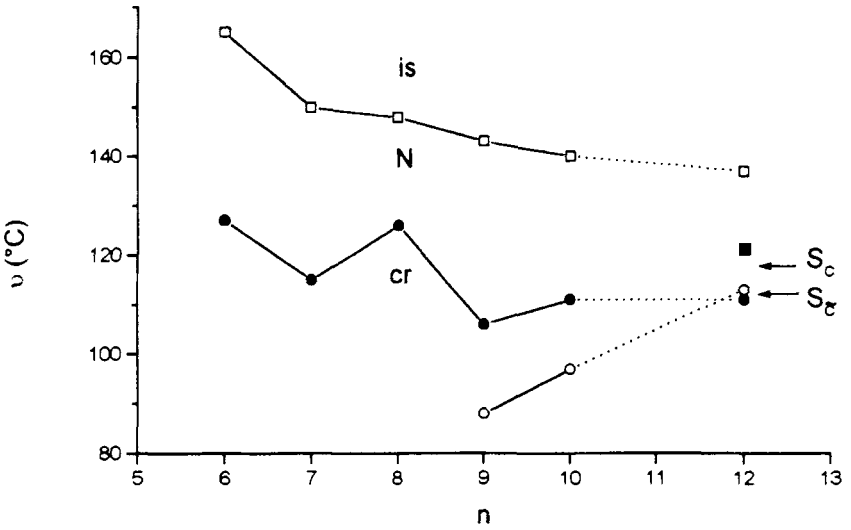

FIGURE 1 Transition temperatures of the homologous series **2a-f**

4. EXPERIMENTAL RESULTS

4.1. Optical investigations and X-ray studies of the mesophases

The transition temperatures of the homologous series **2a-2f** are depicted in Figure 1. For the present, the classification was done by microscopic investigations. The textures seem to be identical with those of nematic and smectic C phases known for calamitic mesogens. That is very unexpected in view of the fact that the novel B phases are reported to be characteristic for mesogens having a bent core. In accordance with that, all five-ring compounds derived from resorcinol or substituted resorcinols, reported in the recent time [4,10], exhibit mesophases of the novel B type. On the other hand, in 1994 AKUTAGAWA et al. [11] reported nematic phases observed for bent five-ring compounds isomeric to the series **2** with the difference that the azomethine groups are inversely inserted.

In the new series the polymorphism $N - smC - sm\tilde{C}$ found for the most long-chained compounds, the dodecyloxy homologue **2f** and the tetradecyl derivative **2g,** is worth mentioning. The phase transition $smC/sm\tilde{C}$ is indicated by a clear texture change (see Figure 2) but up to now it could not be detected by DSC or X-ray investigations.

To support the preliminary phase classification obtained by microscopic studies X-ray measurements were performed in the liquid crystalline state. The patterns of the nematic phase show the feature as known of nematic phase of rod-like compounds exhibiting cybotactic groups, see Figure 3. The sample was hold in glass capillaries. The diffuse scattering in the wide angle region is positioned on the equator of the pattern, which is perpendicular to the magnetic field. That means that the long axis of the molecules are aligned parallel to the field direction. On the other hand, four diffuse scattering maxima in the small angle region indicate the tilt of the molecules within the cybotactic groups. In the case of compound **2c**, e.g., a tilt of 37 degree could be estimated which results in an apparent length of the molecules of 4.5 ± 0.3 nm. The value is smaller than those observed in the crystalline state (L=5.1 nm), but the disorder in the nematic phase should be the reason of the shortening.

The X-ray pattern in the low temperature phase of the compounds **2d** and **2e** exhibits two reflections in the small angle region, the scattering vectors of which are no multiple of each other pointing to a two dimensional structure. Two different orientations have been obtained in dependence on the sample preparation (Figure 4 and Figure 5). Figure 4 follows directly by cooling of the N-phase into the low temperature phase applying a magnetic field. The pattern shows two symmetry axes, along the equator and along the meridian. These two axes can be explained by the experimental conditions: the direction of the capillary axis agrees with the equator and the direction of the magnetic field agrees with the meridian. The pattern indicates that the molecules are aligned parallel to the meridian (parallel to the field) whereas the layer normals are tilted. On the other hand the orientation of a droplet on the glass plate yields the pattern of Figure 5 in which the molecules are inclined with respect to the meridian. Both orientations lead to the same tilt angle of 43 degree. Figure 5b shows the positions of the scattering vectors. Both patterns can be explained by an undulated structure, sketched in Figure 6, like a smC phase with a=4.7 nm, c= 3.6 nm and β=110 degree.

4.2. NMR measurements

NMR investigations were carried out on compounds **2c** and **2f** that differ in the length of the terminal chains. The homologue **2c** exhibits a nematic phase and for

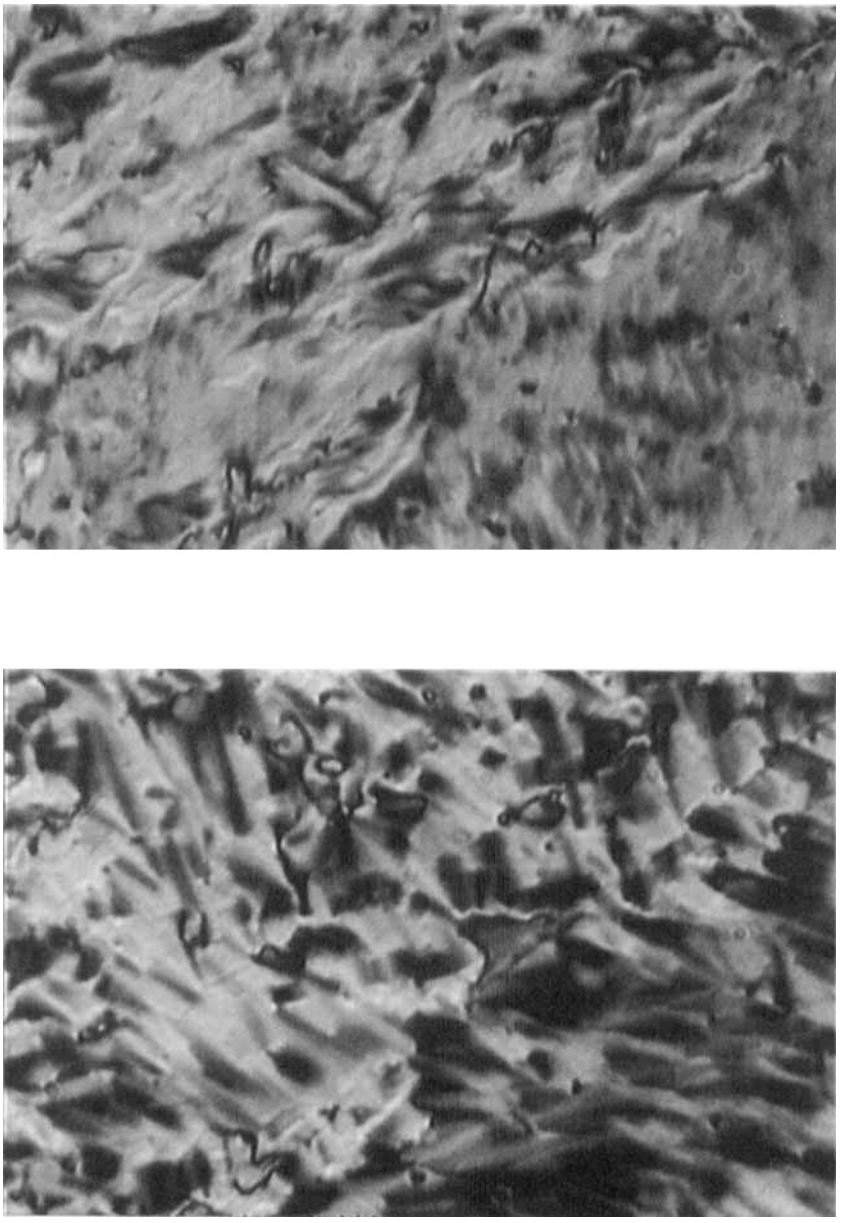

FIGURE 2 Microscopic pictures of compound **2f**: a) smC phase at 113.5 °C; b) $\mathrm{sm}\tilde{\mathrm{C}}$ phase at 110°C (See Color Plate IV at the back of this issue)

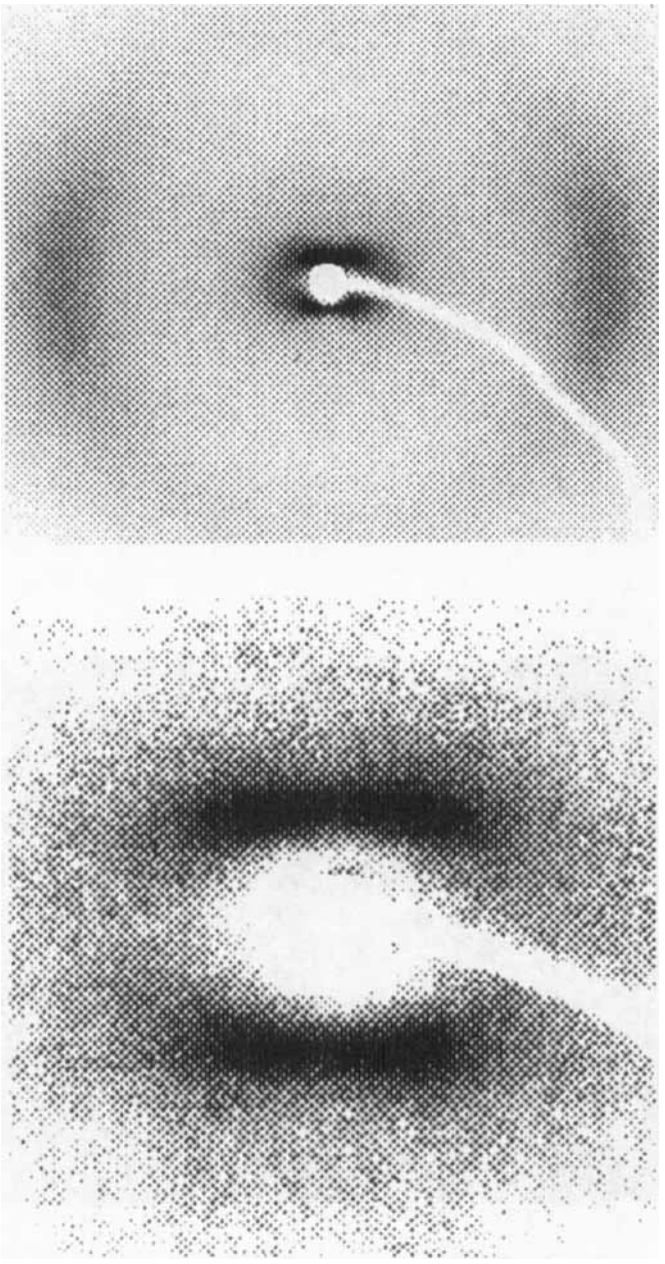

FIGURE 3 X ray pattern of compound **2d** at 120 °C : a) full pattern; b) small angle region

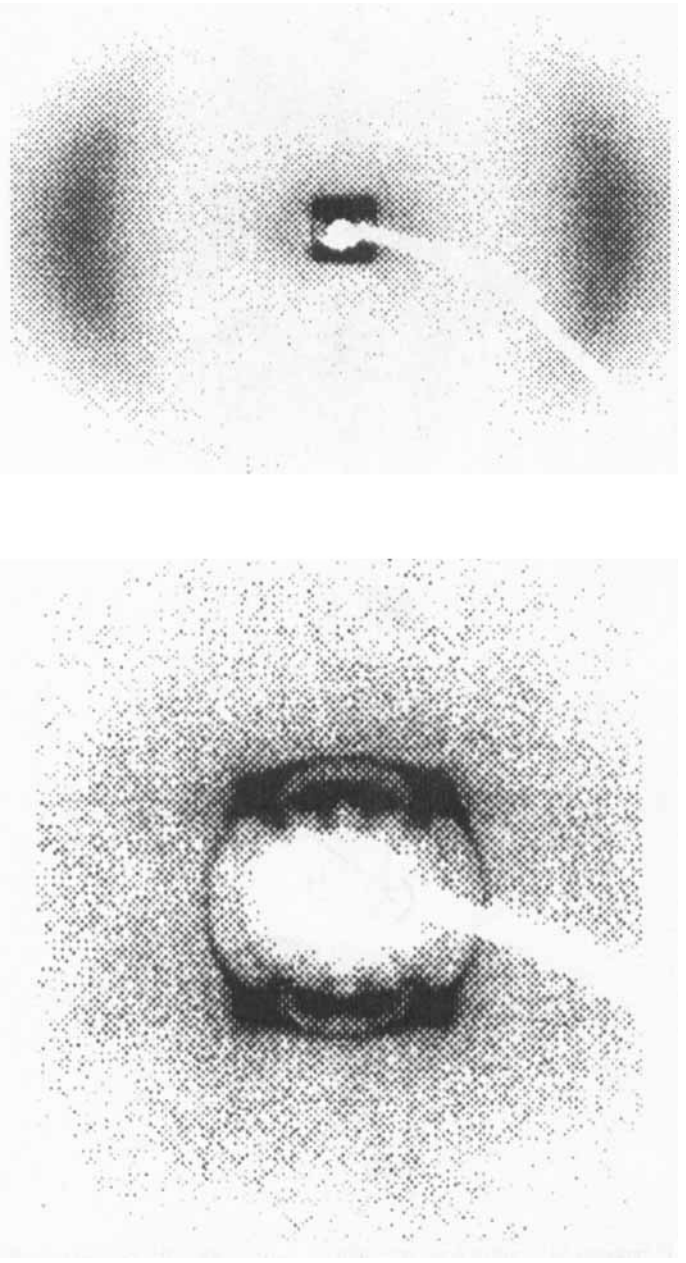

FIGURE 4 X ray pattern of compound **2d** at 82 °C: a) full pattern; b) small angle region

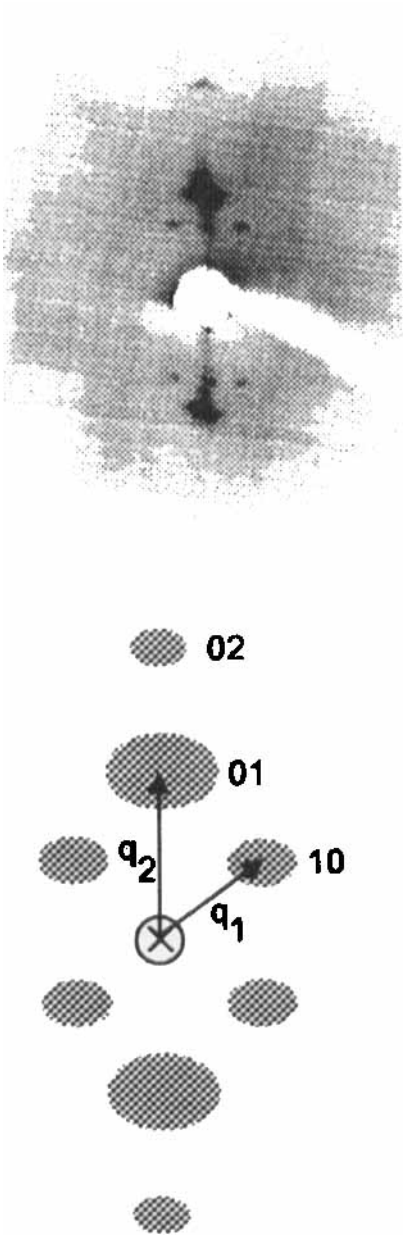

FIGURE 5 Compound **2d**: a) small angle region in the $\mathrm{sm}C$ phase; b) assumed scattering vectors

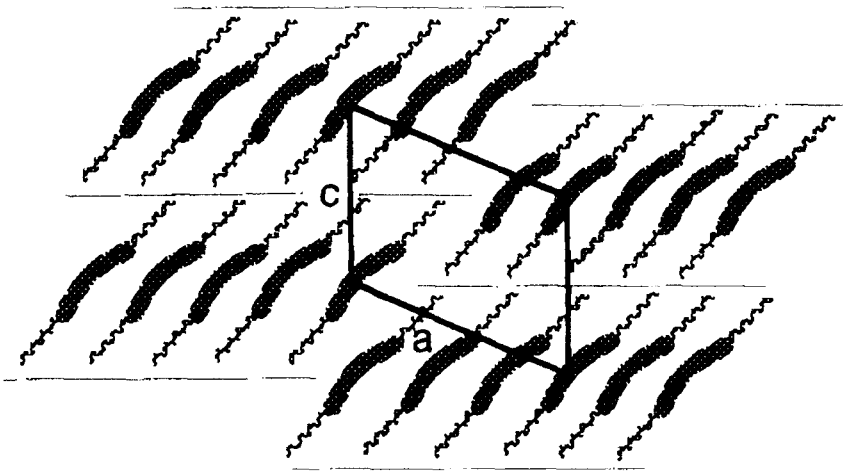

FIGURE 6 Sketch of the undulated structure of the $sm\tilde{C}$ phase under discussion

compound **2f** a nematic - smectic polymorphism is discussed. The numbering of the atoms for the dichlorosubstituted molecules is given in the following formula, also shown is the direction of the molecular long axis.

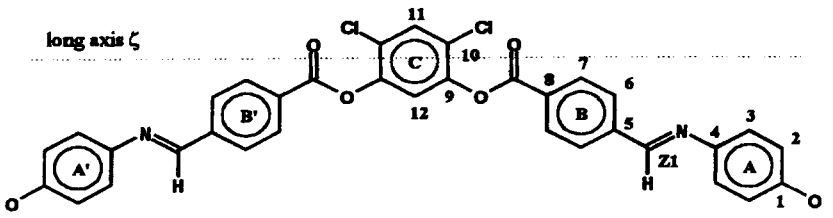

The assignment of the lines in the isotropic spectrum shown in Fig. 7 for **2c** rests upon the increment system and the comparison with other banana-shaped molecules. All carbon positions are resolved only C11 overlaps with C7. All measurements were carried out by decreasing temperatures. The transition to the liquid crystalline phases occurs for both substances within 2K. Fig. 7 shows a spectrum in the nematic phase of **2c.** The lines from C4 and CHN are broadened due to the C-N dipole interaction. One line of the protonated carbons of ring C (C12) overlaps with C2. The line shifts of the aromatic carbons in the liquid crystalline phases increase markedly with decreasing temperature in both derivatives **2c** and **2f.** The lines from carbons belonging to equivalent positions in the two half parts and in the central ring C coalesce permanently in all spectra.

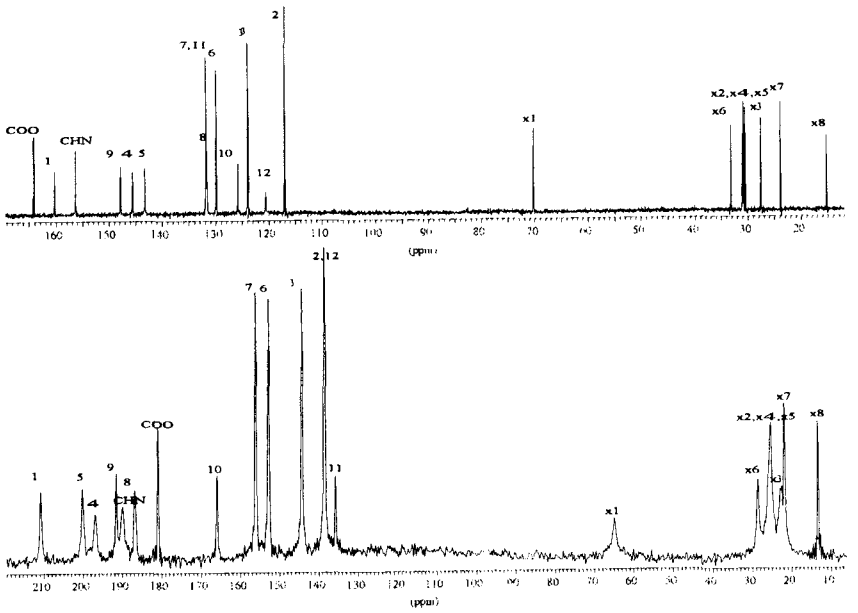

FIGURE 7 Isotropic ^{13}C spectrum of **2c** at 420 K (above) and the spectrum in the nematic phase at 385 K (below). Both spectra are obtained by single pulse exitation and igated Waltz-decoupling

The ^{13}C chemical shift changes can be related to the macroscopic order parameter S by a simple equation

$$\delta^{i}_{obs}(T) = \delta^{i}_{iso} + S\delta^{i}_{\zeta\zeta} \quad (1)$$

Here the small contribution from the biaxality term D is neglected, that has nearly the same small value for all positions. $\delta^{i}_{\zeta\zeta}$ are the components of the shift tensor in the molecular system ξ, η, ζ with ζ as molecular long axis. The symmetry of the spectra demands a direction of the long axis as shown in the chemical formula sketched above. In this system the geometry of the central ring C is well defined. This enables to calculate the order parameter S from the shifts of C9 and C10 if $\delta^{9}_{\zeta\zeta}$ and $\delta^{10}_{\zeta\zeta}$ are known according to equation (1). In accordance with the literature [5,12] $\delta^{9}_{\zeta\zeta}$ =72 ppm (δ^{9}_{11} =91 ppm, δ^{9}_{22} =15 ppm, angle 30° between δ^{9}_{11} and long axis) and $\delta^{10}_{\zeta\zeta}$ =66.2 ppm are used. The value of $\delta^{10}_{\zeta\zeta}$ results from the ratio of the anisotropic shifts of C9 and C10. The obtained order parameter S shown in Figure 8 demonstrates clearly the typical temperature dependence of the ordering, a continuous increase in the nematic phase with an exponent slightly smaller than for classical materials (**2c**) and a jump at the transition to a smectic phase (sample **2f**). The S values are typical for nematic phases

of classical rod-like molecules. The temperature dependence of S in **2f** clearly distinguishes two phases.

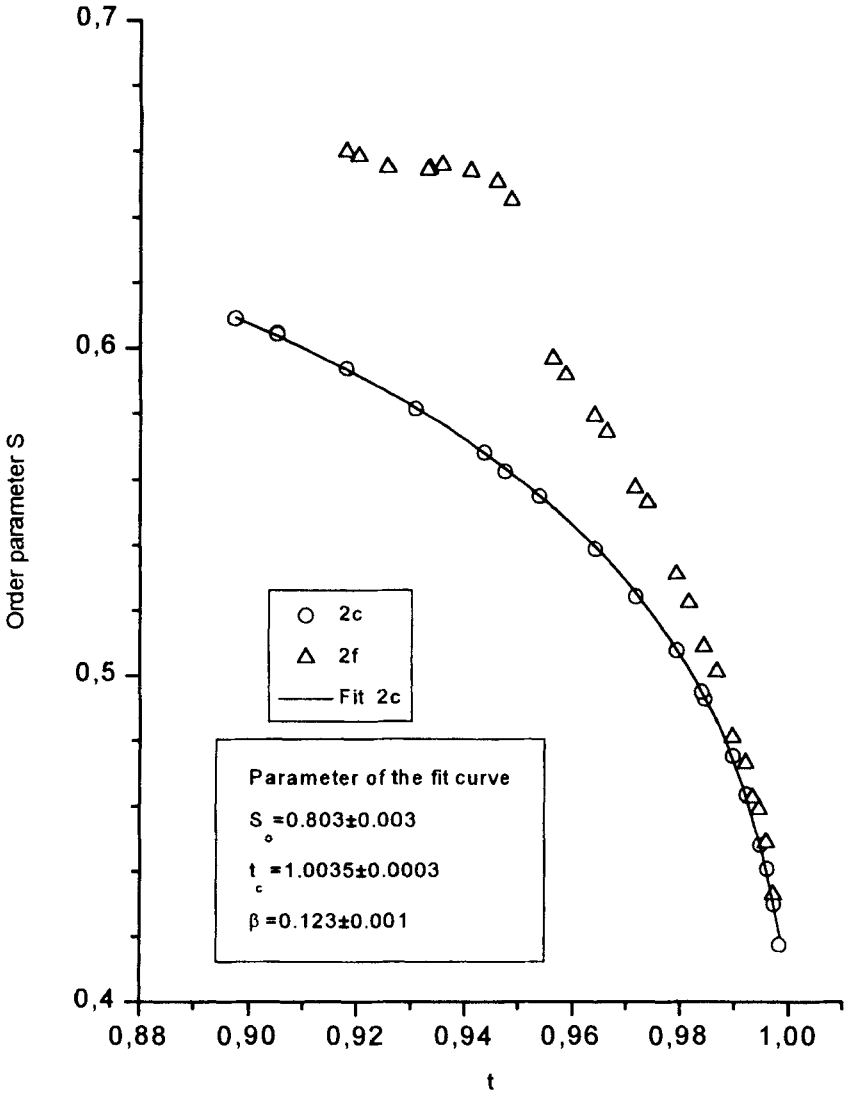

FIGURE 8 Order parameter S for **2c** and **2f** calculated from the shifts of C9 and C10 in the central ring C. The line fits the temperature dependence according to $S = S_o(1- t/t_c)^{\beta}$

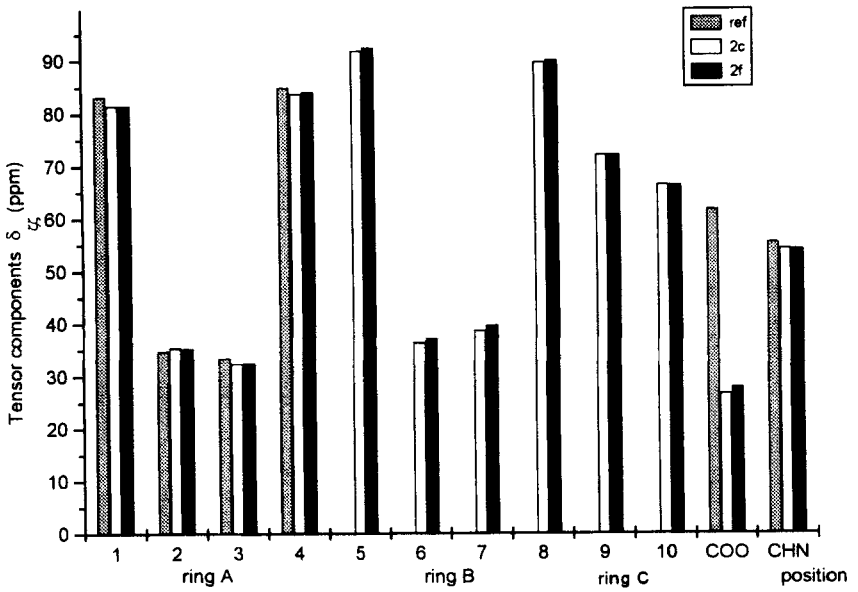

FIGURE 9 The tensor components $\delta^{i}_{\zeta\zeta}$ of the banana-shaped molecules **2c** and **2f** for the carbons i, for a suitable linear reference molecule (CHN) with an identical ring A and a two-ring ester reference substance (COO)

The order parameter describes the ordering of the long molecular axis and is the same for all C atoms of the molecule. Using the S(T) we can extract the $\delta^{i}_{\zeta\zeta}$ (T) for the C^{i} belonging to the rings A, A′ and B, B′ and linkage groups. The results for both substances **2c** and **2f** are given in Figure 9. Included in this figure are also values of a suitable two ring reference material ($C_7H_{15}O$-C_6H_4-CH=N-C_6H_4-OC_8H_{17}: cr 61 (smA 58.5) N 87 is) with $\delta^{l}_{\zeta\zeta}$=84.5 ppm postulated [13]). The second aromatic ring of the reference has the same substituents as ring A in the banana-shaped molecules. Since the isotropic shifts agree exactly their tensor components in the main axes system should also be the same. As seen in Figure 9 the tensor components of the C^{i} from ring A in the chosen molecular system agree with the reference (within an error of ±0.6 ppm). The geometrical relation between the main frame and the molecular frame must be the same for all three molecules. For the linear two ring reference compound the para-axes are nearly aligned with the molecular long axis. The same must be valid for the two molecules under investigation with an error of ±5°. This conclusion is based on the comparison with the reference compound without knowing exactly all three components of the shift tensors. At the moment the same procedure can not be used for ring B. However the observed

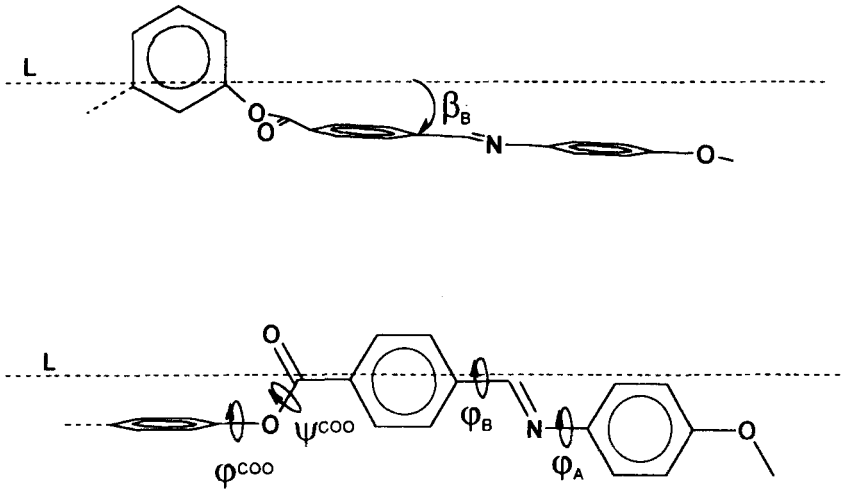

β_B	φ_B	β_A	φ_A	φ^{COO}	ψ^{COO}	φ^{CHN}
5-10°	0-30°	5-10°	40°	110°	30°	65°

FIGURE 10 Conformation of the half-parts for dichlorosubstituted molecules derived from the value of ^{13}C tensor components. The torsion of the ring planes in the picture is arbitrary and does not agree with the estimated values in the table

tensor components have values slightly larger than for ring A, that also allows only small angles between the para- and the long axis. The same is valid for the CHN linkage group. The para-axes of the aromatic rings in both lateral branches align nearly parallel to the molecular long axis, giving the molecules a nearly linear shape. Important for this shape is the geometry of the linkage COO group at ring C. Its tensor component in **2c** and **2f** is noticeably smaller than in the second reference compound (CH_3O-C_6H_4-COO-C_6H_4-OC_6H_{13} cr 56 N 77 is), see Figure 9. A simple torsion of this group and the linked rings around the bond C-O from ring C to ester group (φ^{COO}) would only slightly change the angles of the para-axis of ring B and C. There must be a second rotation around the following bond O-C of the ester group (ψ^{COO}) (Figure 10). Values of 20 to 30° for this angle create a more extended molecule, but now the outer bonds of the ester group no longer form a plane. The measured $\delta^{COO}{}_{\zeta\zeta}$ can be explained by φ^{COO}=110° and a torsion $\psi^{COO}$of ca. 30° around the second bond. The plane of the ester group aligns nearly perpendicular to the plane of ring C (Figure 10).

The close neighbouring chloro substituent favours this torsion and also the second rotation that creates the extended molecular shape.

The strong deformation of the ester linkage group at the dichlorosubstituted ring C generates a nearly linear molecule which form liquid crystalline phases typical for rod-like mesogens. Since peaks of symmetry related to equivalent carbons coincide exactly for all temperatures the observed averaged conformation of the two half-parts is identical beginning with COO linkage group. From NMR measurements there is no possibility to distinguish between a plus and a minus torsion and therefore to obtain information about a fast exchange between the two conformations.

The anisotropic shifts of the carbons belonging to the chains are small, but most peaks in **2c** are resolved in the nematic phase. The values of $(-\delta^{Cx}{}_{\zeta\zeta})$ decrease along the chain from 9 to 3.2 ppm with a smooth increase of each value with decreasing temperature. Because of the smallness the error is large. The comparison with typical values for linear molecules enables us again to conclusions about the chain conformation. The shifts in the slightly bent molecules are 1–2 ppm smaller for equivalent chain positions. A simple model with the assumption of axialsymmetric tensors gives an angle between the chain axis and the long axis which is 15–20° greater than for linear molecules. The smaller value of all shifts beginning with the OCH_2 contradicts a model of a higher flexibility of the chains in these molecules. In this case the decrease of the $(-\delta^{Cx}{}_{\zeta\zeta})$ should increase along the chain.

4.3. Dielectric investigations

Dielectric investigations give information about the dynamics of polar groups or of molecules as a whole. Especially the main processes connected with the reorientation around the short and long molecular axes of whole molecules were intensively investigated in the past [14].

Experimental data of the decyloxy derivative **2e** for the dielectric loss ε'' versus frequency f and temperature υ perpendicular to the director are presented in the 3D-plot of Figure 11. The strong increase of ε'' at low frequencies arises mainly from the conductivity. Furthermore a dielectric absorption at higher frequencies could be detected in the isotropic and the $_{\mathrm{sm}}\tilde{\mathrm{C}}$ phase. The same relaxation range was found also in the parallel direction, but with a quite lower intensity. Therefore, the detected absorption must be connected with the reorientation of the whole molecule around the long molecular axis which is usually detected in the GHz-range. This is shifted to lower frequencies due to the high viscosity of the sample [15]. For the formal description of the experimental data a

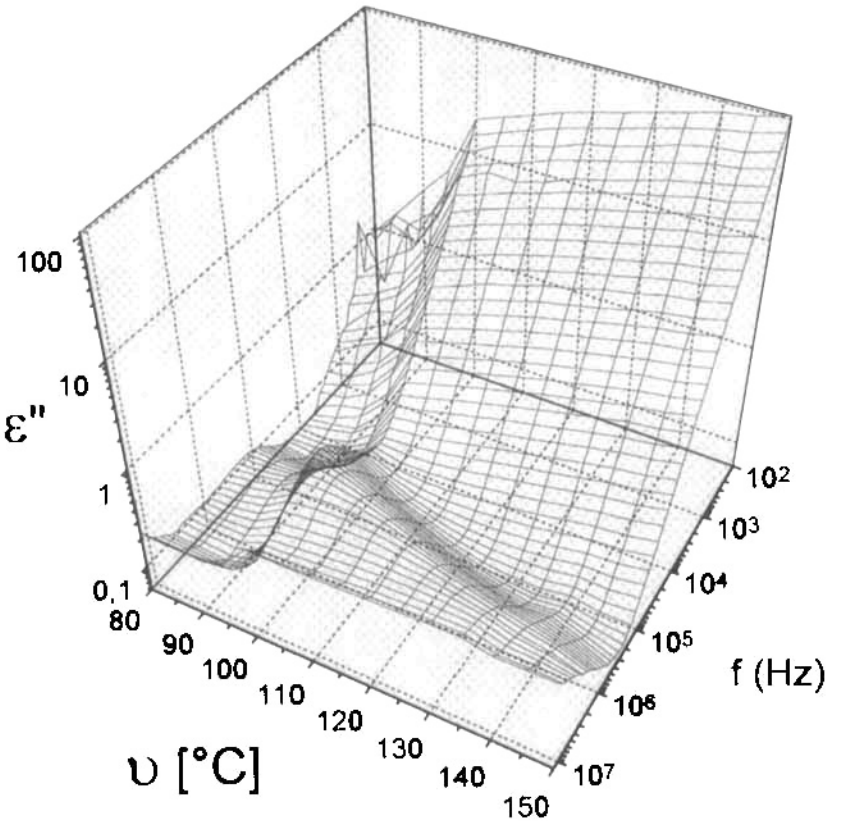

FIGURE 11 3D-plot of the dielectric loss of **2e** versus frequency and temperature perpendicular to the nematic director

COLE-COLE mechanism [16] and a term which considers the conductivity is used:

$$\varepsilon^* = \varepsilon_1 + \frac{\varepsilon_0 - \varepsilon_1}{(1 + j\omega\tau)^{1-\alpha}} + \frac{A}{f^n} \qquad (2)$$

In formula (2) the static dielectric constants ε_0, the high frequency limits ε_1, the relaxation times τ and the COLE-COLE distribution parameter α are parameters of the fit. Experimental data, the fitted curve between 10 kHz and 1 MHz and the fit parameters at $\upsilon = 98$ °C are given in Figure 12. The data were later extended to 4 kHz in order to demonstrate the increase of $\varepsilon_\perp$ due to the formation of an electrical double layer. From the fit at different temperatures characteristic

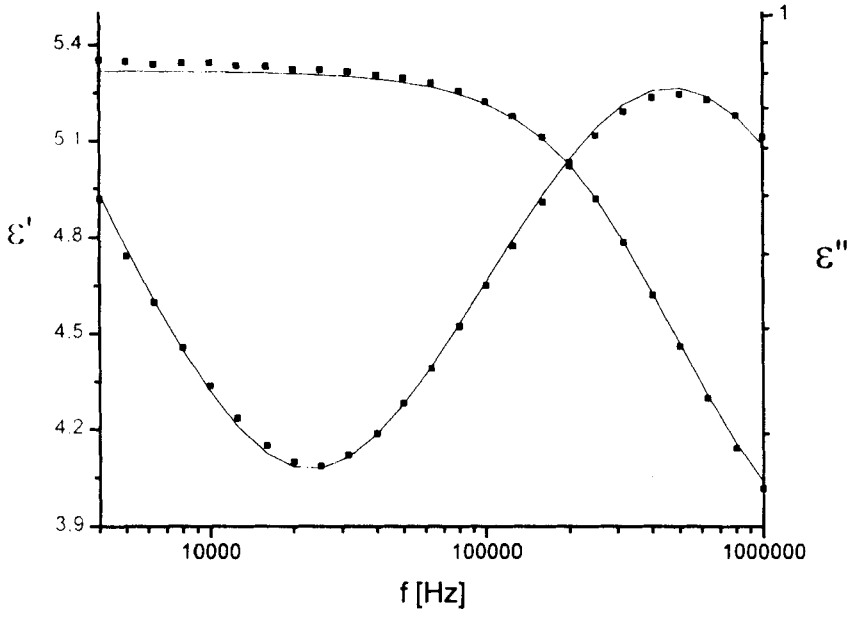

FIGURE 12 Dielectric dispersion and absorption curves of **2e** for the perpendicular direction at υ=98 °C: ε_0=5.32, ε_1=3.69, τ=0.335 μs, α=0.05, A=1.937·10^3 s^{-1}, n=1.00

data for the relaxation process in various phases were obtained. Figure 13 shows the relaxation times versus the reciprocal absolute temperature and the respective dielectric increments $\Delta = \varepsilon_0 - \varepsilon_1$. There is no big change of the relaxation frequencies at the different phase transitions. Additionally, τ-values of the compound **3,** that is 2-chloro-1,3-phenylene bis[4-(4-n-octyloxyphenyliminomethyl) benzoate] (cr 120 B_2 133 is) are given, which contains only one chlorine atom in the middle part [17]. There is a clearly different behavior of the relaxation times at the transition from the isotropic into the liquid crystalline phase. Substance **3** shows a stepwise decrease of the τ about a factor 4. That means the reorientation of the molecules of compound **3** around the long molecular axis is hindered by the ordered curvature of the banana-like molecules in the B_2 phase. This results in the formation of ferroelectric clusters and also in a decrease of the dielectric increment with decreasing temperature [17]. In contradiction to this the reorientation time of sample **2e** is practically not influenced by the phase transition and the dielectric increment increases by cooling the nematic phase. Such a behavior is expected for molecules which can rotate without big hindrance. In conclusion one has to say that the molecules of **2e** exhibit a nearly rod-like shape.

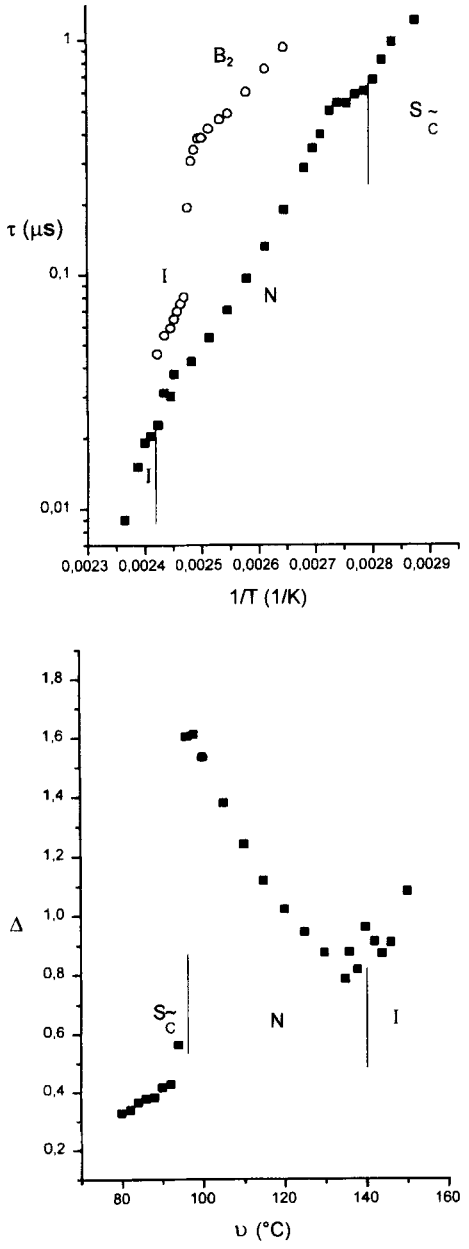

FIGURE 13 a) Relaxation times τ of the dichlorosubstituted compound **2e** (squares) and the comparable monochlorosubstituted octyloxy derivative **3** (circle) as function of the reciprocal absolute temperature. The activation energy in the N-phase is (83±4) $kJmol^{-1}$. b) Dielectric increments of compound **2e** at different temperatures

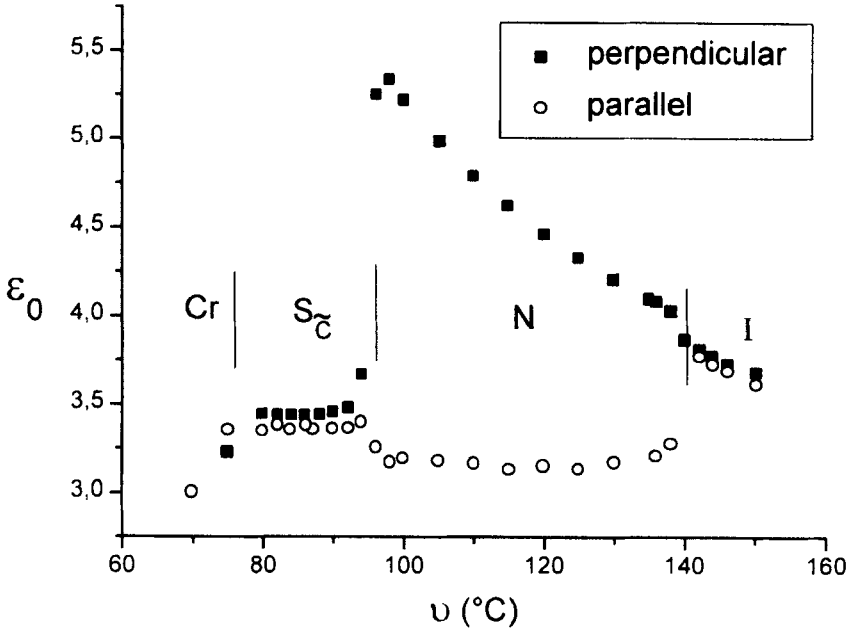

FIGURE 14 Static dielectric constants of sample **2e** as function of the temperature

The plot of the static dielectric constants at different temperatures in Figure 14 looks like that of a normal nematic compound with a negative dielectric anisotropy. The strong decrease of $\varepsilon_{\perp 0}$ and the increase of $\varepsilon\|_0$ at the phase transition below 100 °C can be interpreted as transition into a phase where the molecules are tilted. This phase should not exhibit a herring-bone structure, because then the reorientation around the long axis shown in Figure 13 should change stepwise.

4.4. Electrooptical investigations

The planar oriented nematic phase of the octyloxy derivative **2c** exhibits two-dimensional domains on applying a d.c. field or a low frequency field, see Figure 15a. The threshold in a 6 μm thick cell is 15 V for a d.c. voltage (135 °C) and increases with increasing frequency. These domains obviously correspond to the conductive regime of electrohydrodynamic instabilities.

At 1 kHz above 60 V a new type of domains appear. These domains are perpendicular to the original director orientation but their period is 2.5 – 3 times larger than the sample thickness. The threshold clearly increases with increasing

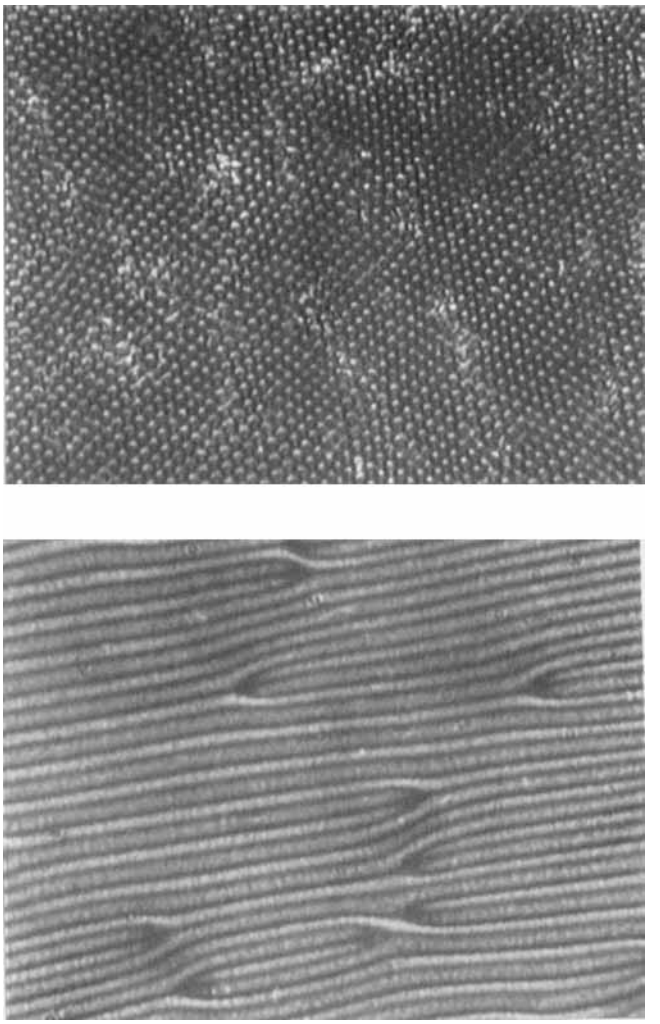

FIGURE 15 a) Two-dimensional domains in the nematic phase of compound **2c**; temperature: 135 °C; sample thickness: 6 μm; applied voltage: 16 V (30 Hz). b) a.c. domains in the nematic phase of compound **2c**; temperature: 135 °C; sample thickness: 6 μm; applied voltage: 85 V (3 kHz); period of domains: 16 μm. The domains are perpendicular to the original direction of the director (See Color Plate V at the back of this issue)

frequency, for a frequency of 4 kHz a threshold of 80 V was found for a sample thickness of 6 μm (135°C).

Under microscopic observation between crossed polarizers the domains appear as alternating red and green bands almost equal in width (see Figure 15b). These

domains are perpendicular to the original director direction. The stripe pattern is best visible when the polarizer is parallel to the unperturbed planar orientation. Such type of domains were predicted by Pikin and Chigrinov [18] and experimentally described by Trufanov et al. [19] and Weissflog et al. [20]. The domain pattern can be interpreted as inertia mode of electrohydrodynamic instabilities which correspond to a steady state motion of the liquid crystal and stationary deviations of the director.

4.5. Single crystal X-ray investigations

Molecular structure

The molecular structure of **2c** is illustrated by a thermal motion plot in Fig. 16. A realistic picture of the molecular shape can be visualized by the space filling model shown in Fig. 17 for which the van der Waals radii given by Bondi [21] were used. Essential parameters of the molecular geometry are summarized in Tables III and IV. The atom labelling scheme used is based on the fact that the molecule is symmetric in the sense of its chemical constitution, i.e. it consists of two chemically equal halves. The two atoms common to both halves are C1 and C4 whereas equivalent atoms belonging to the left side and to the right side of the molecule are labelled as C2, C3, O1 ... and C2′, C3′, O1′ ..., respectively (cf. Fig. 16).

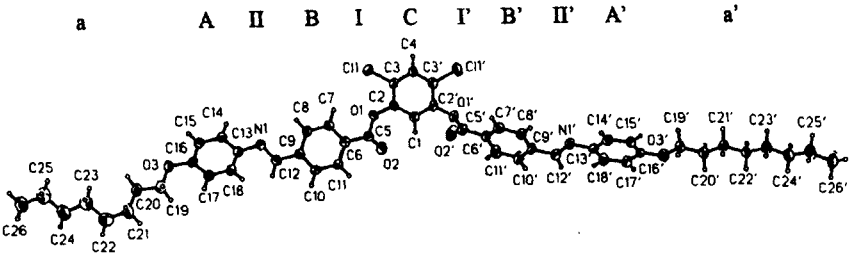

FIGURE 16 Molecular structure of **2c** with the atom labeling used in the X-ray analysis (displacement parameters at the 50% probability level, arbitrary size of H atoms)

In contrast to its chemical constitution, the molecule is rather far from mirror symmetry with respect to its geometry. The two molecular halves differ markedly in some points. The molecule as a whole is not planar but it consists of structural fragments with more or less perfect planarity. All five benzene rings A to A′ as well as the two carboxyl groups (i.e. their C-CO.O moieties) I and I′ are planar within 3σ. Also the left side azomethine moiety II (its l.s. plane is defined

by the four atoms C9, N1, C12, C13) is exactly planar but its right side equivalent II′ is slightly uneven with a maximum deviation of 0.044(3) Å for C12′.

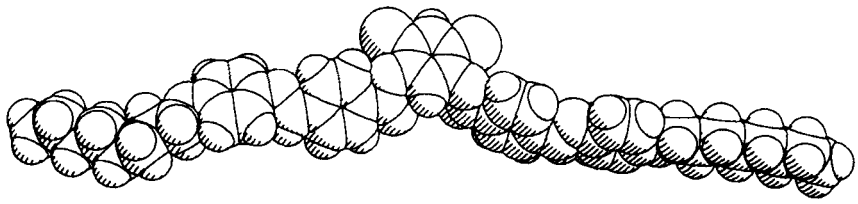

FIGURE 17 Space filling plot of the molecule (atom spheres according to the van der Waals radii given by Bondi [21])

Of special interest is the conformation of the central 1,3-phenylene bis(benzoate) moiety. Phenyl benzoate is a very common component of thermotropic mesogens [22] and its structure has been investigated in many cases. In general, the orientation of the C- and O-bonded benzene rings with respect to the bridging carboxyl group is approximately parallel and perpendicular, respectively. The special values of 0° and 90° for the corresponding dihedral angles were found in 4-cyanophenyl 4-n-pentoxybenzoate [23] which has exact C_s symmetry whereas in the unsubstituted phenyl benzoate 9.8° and 65.1° were observed [24] and in all other cases the dihedral angles are widely scattered over the ranges 0 to about 15° and 90 to about 60°, respectively. Thus the dihedral angles of the right side I′/B′ = 9.8(3), I′/C = 82.7(2), and B′/C = 73.7(2)° agree with expectation but the dihedral angles of the left side being I/B = 14.3(3), I/C = 47.8(2), and B/C = 33.6(2)° are quite unusual. (The conformational behavior just and in the following discussed by means of the dihedral angles can be described in an equivalent manner by the appropriate torsion angles given in Table IV, of course).

Also the two benzylideneaniline moieties of **2c** differ considerably in their conformational behaviour. The twist of the C-C bonded benzene ring with respect to the four-atom azomethine plane (see above) is rather small and exactly the same for the left and right side of the molecule, the corresponding dihedral angles amount to 13.6(8) and 13.8(4)°, respectively. In contrast to that, disagreement of the twist of the C-N bonded phenyl rings (A/II = 36.4(4) and A′/II′ = 19.0(4)°) is observed and the two angles between the benzene ring planes being A/B = 49.6(2) and A′/B′ = 14.8(2)° differ strongly. As a result of theoretical studies, a marked non-planarity has been proved to be the preferred conformation of benzylideneanilines. *Ab initio* calculations indicated that the minimum energy conformation corresponds to a rotation about the N-phenyl bond of 45° and a rotation about the C-phenyl bond of 0° [25]. But our data for **2c** as well as a great

number of X-ray structural data estimated for other benzylideneanilines (cf. the discussion of the problem in [26]) show a large scatter and demonstrate the strong influence of crystal packing forces on the molecular conformation in this case.

Finally, also the two octyloxy wing groups differ remarkably in their conformations. The left side octyloxy chain includes a *gauche* conformation (characterized by the torsion angle C20-C21-C22-C23 = −67.4(6)°) and its O3...C22 fragment is inclined by 18.7(4)° to benzene ring A. In contrast to that, the right side octyloxy chain is in all-*trans*-conformation and only slightly inclined by 1.5(2)° to benzene ring A′.

At the moment we can offer no other possible explanation for the anomalies in the conformational behavior and the drastic differences between left and right side in **2c** than crystal packing forces.

TABLE III Selected bond lengths (A) and angles (°) in (esd's in parentheses)

Atoms	*Distance*		*Atoms*	*Angle*	
	left side[a)]	*right side*[a)]		*left side*[a)]	*right side*[a)]
C3-C11	1.732(5)	1.731(5)			
		Carboxyl group			
C2-O1	1.388(6)	1.398(6)	C2-O1-C5	119.8(4)	115.9(4)
O1-C5	1.336(6)	1.375(6)	O1-C5–02	123.5(5)	122 2(5)
C5-O2	1.192(6)	1.192(6)	O1-C5-C6	110.7(4)	111.2(5)
C5-C6	1.478(7)	1.484(7)	O2-C5-C6	125.8(5)	126.5(5)
		Azomethine group			
C9-C12	1.465(7)	1.470(7)	C9-C12-N1	121.7(5)	123.0(5)
C12-N1	1.270(6)	1.257(6)	C12-N1-C13	119.7(5)	120.0(5)
N1-C13	1.423(6)	1.428(6)			
		Octyloxy group			
C16-O31	1.373(6)	1.372(6)	C16-O3-C19	117.8(4)	119.0(4)
O3-C19	1.429(6)	1.434(6)	C-C-C (mean)	111.4(1.6)	113.8(1.7)
C-C (mean)	1.536(11)	1.516(8)			
		Mean values for benzene rings			
		Ring A (C13...C18)			
C-C (mean)	1.381(7)	1.385(7)	C-C-C (mean)	120.0(8)	120.0(1.9)
		Ring B (C6...C11)			
C-C (mean)	1.383(11)	1.384(6)	C-C-C (mean)	120.0(1.0)	120.0(1.0)
		Ring C(C1...C2′)			
C-C (mean)	1.379(7)		C-C-C (mean)	120.0(9)	

a) The terms "left side" and "right side" refer to the presentation of the molecular structure given in figure 1, i.e. "left side" atoms are C3, C2, O1 ... C26 and " right side" atoms are C3′, C2′, O1′... C26′.

TABLE IV Selected torsion angles (°)

Atoms	*Torsion angle*	
	left side[a)]	*right side*[a)]
C1-C2-O1-C5	-53.8(7)	87.9(6)
C3-C2-O1-C5	129.7(5)	-95.0(6)
C2-O1-C5-O2	6.9(8)	-8.0(8)
C2-O1-C5-C6	-172.4(4)	170.0(4)
O1-C5-C6-C7	15.1(7)	-9.4(8)
O1-C5-C6-C11	-167.8(5)	173.6(5)
O2-C5-C6-C7	-164.3(5)	168.4(6)
O2-C5-C6-C11	12.9(8)	-8.5(9)
C8-C9-C12-N1	11.3(8)	-12.5(9)
C10-C9-C12-N1	-165.6(5)	165.0(6)
C9-C12-N1-C13	179.9(5)	-172.4(5)
C12-N1-C13-C14	-144.9(5)	-165.3(5)
C12-N1-C13-C18	37.5(8)	18.2(8)
C15-C16-O3-C19	172.7(5)	3.8(7)
C20-C21-C22-C23	-67.4(6)	-176.4(5)

a) The terms "left side" and "right side" refer to the presentation of the molecular structure given in figure 1, i.e. "left side" atoms are C3, C2, O1 ... C26 and "right side" atoms are C3′, C2′, O1′ ... C26′.

As can be seen in Figures 16 and 17, the molecule has a banana shape but this is essentially less pronounced than originally expected. The bend of the molecular long axis can be described by differently defined angles. At the first sight, the substitution of the 1,3-positions in the central benzene ring gives rise to a bend angle of 120°. But the actual conformations of the bridging groups and the octyloxy chains lead to a drastic reduction of the bend which can be illustrated by the following bend angles: The two lines connecting the centroids of rings B and C on the one hand and B′ and C on the other hand make an angle of 123.9° but the analogously defined angle A-C-A′ is 147.1° and the lines connecting the molecular ends (atoms C26 and C26′, respectively) and the centre of benzene ring C include an angle of 155.5°. A noticeable contribution to the unexpectedly small molecular bend is made by the *gauche* conformation of octyloxy chain a.

The observed bond lengths and angles for non-hydrogen atoms (Table III) are quite normal and agree well with appropriate standard values [27]. Corresponding values of the left and right side of the molecule are equal within experimental error (3σ criterion) with the only exception of bond angles C2-O1-C5 and C2′-O1′-C5′ which differ by 3.9(4)°.

TABLE V Crystal data and details of the X-ray structure analysis of compound **2c**

Empirical formula	$C_{50}H_{54}Cl_2N_2O_6$
Molecular weight (g mol^{-1})	849.85
Crystal system	triclinic
Space group	$P\bar{1}$
Lattice parameters	
a (Å)	12.164(2)
b (Å)	14.006(2)
c (Å)	14.327(3)
α(°)	92.38(2)
β(°)	97.97(2)
γ(°)	112 38(1)
V ($Å^3$)	2223.4(7)
Z	2
F(000)	900
D_c (g cm^{-3})	1.269
μ(MoK_α) (mm^{-1})	0.198
Crystal size (mm)	0.270 × 0.207 × 0.080
Check reflections	3
Max. intensity variation (%)	9.9
$2\Theta_{max}$ (°)	24.93
hkl range	$\bar{14}$, $\bar{16}$, $\bar{16}/14$, 16, 16
Measured reflections	15741
Independend reflections	7777
R_{int}	0.1158
Observed reflections, $I > 2\sigma(I)$	3858
Refined parameters	541
Weighting coefficients *a*/*b*[a)]	0.0336/1.9453
$\Delta\rho_{fin.}$ (min./max.) (e $Å^{-3}$)	0.400/-0.373
*R*1/*wR*2/*S* (observed data)	0.0778/0.1284/1.246
*R*1/*wR*2/*S* (all data)	0.1864/0.1816/1.158

a) $w=[\sigma^2(F_0^2)+(a\cdot P)^2+b\cdot P]^{-1}$ where $P=(F_0^2+2F_c^2)/3$.

TABLE VI Final fractional coordinates and equivalent displacement parameters ($Å^2$) of 4,6-dichloro-1,3-phenylene bis[4-(4-n-octyloxyphenyliminomethyl) benzoate] **2c**

Atom	*x/a*	*y/b*	*z/c*	U_{eq}	*Atom*	*x/a*	*y/b*	*z/c*	U_{eq}
C1	0.7057(4)	0.9587(4)	0.7090(4)	0.036(1)	C11	0.4879(1)	0.6616(1)	0.7051(1)	0.045(1)
C2	0.6069(4)	0.8689(4)	0.7141(3)	0.033(1)	C2′	0.8060(4)	0.9508(4)	0.6826(4)	0.034(1)
C3	0.6101(4)	0.7728(4)	0.6927(3)	0.031(1)	C3′	0.8084(4)	0.8548(4)	0.6592(3)	0.036(1)
C4	0.7098(4)	0.7650(4)	0.6638(3)	0.034(1)	C5′	0.9890(5)	1.0824(4)	0.7562(4)	0.041(1)
C5	0.4998(5)	0.9263(4)	0.8154(4)	0.035(1)	C6′	1.1007(4)	1.1649(4)	0.7362(4)	0.034(1)
C6	0.3754(5)	0.9050(4)	0.8308(4)	0.033(1)	C7′	1.1248(5)	1.1848(4)	0.6458(4)	0.037(1)
C7	0.2755(4)	0.8201(4)	0.7837(4)	0.036(1)	C8′	1.2341(4)	1.2572(4)	0.6320(4)	0.036(1)
C8	0.1632(5)	0.8003(4)	0.8048(4)	0.042(1)	C9′	1.3215(4)	1.3120(4)	0.7092(4)	0.036(1)
C9	0.1461(5)	0.8643(4)	0.8733(4)	0.034(1)	C10′	1.2957(5)	1.2950(4)	0.7992(4)	0.048(2)
C10	0.2442(5)	0.9495(4)	0.9181(4)	0.045(2)	C11′	1.1873(5)	1.2214(4)	0.8138(4)	0.045(2)
C11	0.3581(5)	0.9698(4)	0.8979(4)	0.044(2)	C12′	1.4427(5)	1.3847(4)	0.6986(4)	0.040(1)
C12	0.0278(5)	0.8397(4)	0.9015(4)	0.039(1)	C13′	1.6060(4)	1.4527(4)	0.6195(4)	0.033(1)
C13	-0.1716(5)	0.7316(4)	0.9055(3)	0.035(1)	C14′	1.6391(5)	1.4749(4)	0.5315(4)	0.037(1)
C14	-0.2365(5)	0.6310(4)	0.9255(4)	0.037(1)	C15′	1.7565(5)	1.5283(4)	0.5200(4)	0.036(1)
C15	-0.3465(5)	0.6066(4)	0.9536(4)	0.039(1)	C16′	1.8454(4)	1.5624(4)	0.5995(4)	0.031(1)
C16	-0.3951(5)	0.6807(4)	0.9608(4)	0.034(1)	C17′	1.8160(5)	1.5441(4)	0.6891(4)	0.038(1)
C17	-0.3323(5)	0.7804(4)	0.9393(4)	0.037(1)	C18′	1.6970(5)	1.4897(4)	0.6985(4)	0.042(1)
C18	-0.2211(5)	0.8045(4)	0.9117(3)	0.037(1)	C19′	2.0075(4)	1.6377(4)	0.5106(4)	0.038(1)
C19	-0.5515(5)	0.7244(4)	1.0115(5)	0.050(2)	C20′	2.1426(5)	1.6935(4)	0.5355(4)	0.041(1)

Atom	*x/a*	*y/b*	*z/c*	U_{eq}	*Atom*	*x/a*	*y/b*	*z/c*	U_{eq}
C20	-0.6570(5)	0.6762(4)	1.0629(4)	0.052(2)	C21′	2.2082(4)	1.7292(4)	0.4523(4)	0.039(1)
C21	-0.7149(4)	0.7554(3)	1.0753(4)	0.082(2)	C22′	2.3443(4)	1.7838(4)	0.4856(4)	0.038(1)
C22	-0.7999(4)	0.7275(4)	1.1491(4)	0.105(3)	C23′	2.4172(5)	1.8283(4)	0.4085(4)	0.045(2)
C23	-0.9129(4)	0.6277(4)	1.1157(3)	0.074(2)	C24′	2.5503(5)	1.8840(4)	0.4455(4)	0.048(2)
C24	-1.0015(4)	0.6043(4)	1.1869(4)	0.078(2)	C25′	2.6250(5)	1.9365(5)	0.3726(5)	0.061(2)
C25	-1.1141(3)	0.5040(3)	1.1542(3)	0.092(3)	C26′	2.7566(5)	1.9995(5)	0.4133(6)	0.082(2)
C26	-1.1978(3)	0.4758(3)	1.2290(3)	0.083(2)	N1′	1.4828(4)	1.3895(3)	0.6219(3)	0.035(1)
N1	-0.0583(4)	0.7521(3)	0.8764(3)	0.038(1)	O1′	0.9062(3)	1.0403(3)	0.6747(2)	0.039(1)
O1	0.4993(3)	0.8696(3)	0.7353(2)	0.039(1)	O2′	0.9708(4)	1.0519(3)	0.8313(3)	0.062(1)
O2	0.5897(3)	0.9837(3)	0.8654(3)	0.053(1)	O3′	1.9666(3)	1.6123(3)	0.5990(2)	0.041(1)
O3	-0.5041(3)	0.6482(3)	0.9920(3)	0.042(1)	C11′	0.9369(1)	0.8469(1)	0.6270(1)	0.053(1)

Molecular packing

The molecular packing of **2c** within the crystal is characterized by a perfectly parallel alignment of the molecular long axes generated by the three lattice translations and the inversion centres of the space group (Figure 18). The molecules are arranged parallel in lamellar sheets $(1\bar{1}4)$. Within the sheets the molecules are strongly intercalated as illustrated in Figure 19. Crystal data and relevant details of structure determination and refinement are given in Table V. Final atomic parameters are given in Table VI.

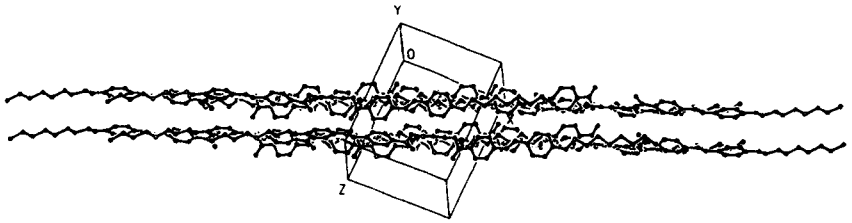

FIGURE 18 Plot of the crystal packing of **2c** showing two lamellar sheets

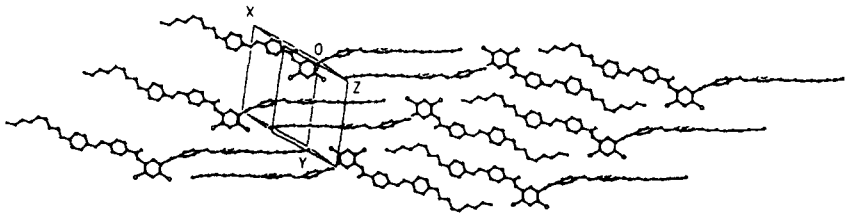

FIGURE 19 One lamellar sheet of molecules aligned parallel $(1\bar{1}4)$ (the other inversion-related sheet is omitted for clarity)

Judging from the observed non-hydrogen intermolecular atomic distances, there is no indication of other than normal van der Waals forces within the crystal lattice.

5. CONCLUSIONS

The investigation of non-chiral banana-shaped mesogens is of topical interest because of their novel mesophases, and especially, their ferro- or antiferroelectric behaviour. For the specific synthesis of such compounds the question arises:

which chemical constitution should the molecules exhibit to form the novel B phases? All appropriate compounds reported in the literature, yet, contain the 1,3-phenylene unit in the centre of the molecules. However, not in all instances the bending angle of 120 degrees resulting from this central part is transmitted on the two half-parts of the molecules. The conformational flexibility of the connecting groups between the aromatic rings as well as the terminal alkyl chains allows an increase (or decrease) of the bending angle which can be slightly changed up to the terminal ends. A further aspect can be the substitution of the central phenyl ring by different atoms or groups, which have also a great influence on the bending angle [4]. The introduction of one chlorine atom in position 4 results in banana-shaped liquid crystals exhibiting the B_2 phase [17]. However, as shown in the paper under discussion, two chlorine atoms attached to the positions 4 and 6 of the central ring change the shape of the molecules dramatically: the resulting five-ring mesogens are not banana-shaped molecules but have a nearly stretched conformation. The bending angle between the two half-parts is about 165° so that these compounds can be regarded as calamitic ones which form nematic or usual smectic phases ((smC, $\mathrm{sm}\tilde{\mathrm{C}}$) . The assignment of the phases is supported by optical and X-ray studies. NMR investigations within the liquid crystalline state confirm the results of a stretching of the molecules caused by the rotation of the molecular fragments around the O-CO bonds which are linked to the central phenyl ring. Semiempirical AM1 and PM3 calculations were performed for selected conformers within the gas phase to quantify energetically the electronic and steric effects of the two neighbouring chlorine atoms. However, energy difference less than 1.0 kcal/mol were found which is not enough to conclude about the molecular shape in the condensed phase.

The dynamic behaviour is comparable to that known for calamitic compounds: the relaxation time related to the rotation of the molecules around the long axes is changed continuously at the transition points between the different mesophases. The relatively stretched shape of the molecules could be also proved for the crystalline state.

The experimental facts presented here lead to the conclusion that – concerning the chemical constitution – the boundary between calamitic mesogens which form nematic and smectic phases and bent mesogens which form the novel B phases is very small.

Acknowledgements

The authors thank the "Deutsche Forschungsgemeinschaft" and the "Fonds der chemischen Industrie" for the support of this work. Many thanks to Prof. Dr. W. Friedrichsen, University of Kiel, for the semiempirical calculations.

References

[1] T. Niori, F. Sekine, J. Watanabe, T. Furukawa and H. Takazoe, *J. Mater. Chem.* **6**, 1231 (1996).
[2] H.R. Brand, P. Cladis and H. Pleiner, *Macromolecules* **25,** 7223 (1992).
[3] D.R. Link, G. Natale, R. Shao, J.E. Maclennan, N.A. Clark, E. Körblova and D.M. Walba, *Science* **278,** 1924 (1997).
[4] W. Weissflog, Ch. Lischka, I. Benné, T. Scharf, G. Pelzl, S. Diele and H. Kruth *Proc. SPIE* **Vol. 3319,** 14–19 (1998); S. Diele, S. Grande, A. Jakli, H. Kruth, Ch. Lischka, G. Pelzl, W. Weissflog and I. Wirth, *17th International Liquid Crystal Conference,* Strasbourg, 20.-24.7.1998, Abstracts D2–04, p. O-30.
[5] S. Diele, S. Grande, H. Kruth, Ch. Lischka, G. Pelzl, W. Weissflog and I. Wirth, *Ferroelectrics,* **212,** 169 (1998).
[6] B. Neises and W. Steglich, *Angew. Chem.* **90,** 556 (1978).
[7] G.M. Sheldrick, *SHELXS-86, Acta Crystallogr.,* **A46,** 467 (1990).
[8] G.M. Sheldrick, 1993, *SHELXL-93, Program for the refinement of crystal structures,* University of Göttingen, Germany, (1993).
[9] XP/PC, *Molecular graphics program package for display and analysis of stereochemical data,* Version 4.2. for MS-DOS, Siemens Analytical X-ray Instruments, Inc., Madison, USA (1990).
[10] T. Sekine, Y. Takanishi, T. Niori, J. Watanabe and H. Takazoe, *Jpn. J. Appl. Phys.* **36,** L 1201–1203 (1997).
[11] T. Akutagawa, Y. Matsunaga and K. Yasuhara, *Liq. Crystals* **17,** 659 (1994).
[12] T.M. Duncan, *A compilation of chemical shift anisotropies,* The Farragut Press, Madison, 1990.
[13] A. Riede, S. Grande, A. Hohmuth and W. Weissflog, *Liq. Crystals* **22,** 157 (1997).
[14] H. Kresse, "Dielectric Behavior of Liquid Crystals", *Adv. Liq. Cryst.* (ed. G. H. Brown) **6,** 109 (1983).
[15] H. Kresse, S. Ernst, W. Wedler, D. Demus and F. Kremer, *Ber. Bunsengesell. Phys. Chem.* **94,** 1478 (1990).
[16] N.R. Hill, W.E. Vaughan, A.H. Price and M. Davies, *Dielectric Properties and Molecular Behaviour* (van Nostrand Reinhold) 1946.
[17] G. Pelzl, S. Diele, S. Grande, A. Jakli, Ch. Lischka, H. Kresse, H. Schmalfuss, I. Wirth and W. Weissflog, *Liq. Crystals,* **26,** 401 (1999).
[18] S.A. Pikin and V.G. Chigrinov, *Zh. Eksp. Teor. Fiz.* **78,** 246 (1980).
[19] A.N. Trufanov, L.M. Blinov and M.I. Barnik, *Zh. Eksper. Teor. Fiz.* **78,** 622 (1980).
[20] W. Weissflog, G. Pelzl, H. Kresse and D. Demus, *Cryst. Res. Technol.* **23,** 1259 (1988).
[21] A. Bondi, *J. Phys. Chem.,* **68,** 441 (1964).
[22] (a) D. Demus, H. Demus and H. Zaschke, 1974, *Flüssige Kristalle in Tabellen* (Deutscher Verlag fiir Grundstoffindustrie, Leipzig, 1974); (b) D. Demus and H. Zaschke., *Flüssige Kristalle in Tabellen II* (Deutscher Verlag für Grundstoffindustrie, Leipzig, 1984).
[23] U. Baumeister, H. Hartung, M. Gdaniec and M. Jaskólski, *Mol. Cryst. Liq. Cryst.,* **69,** 119 (1981).
[24] J.M. Adams and S.F. Morsi, *Acta Crystallogr.,* **B32,** 1345 (1976).
[25] J. Bernstein, J.M. Engel, and A.T. Hagler, *J. Chem. Phys.,* **75,** 2346 (1981).
[26] R. Boese, M.Yu. Antipin, M. Nussbaumer and D. Bläser, *Liq. Crystals,* **12,** 431 (1992).
[27] P. Rademacher, *Strukturen organischer Moleküle* (VCH Verlagsgesellschaft mbH, Weinheim, 1987).